

# Investigating the Characterization and Grindability Behaviour of Farin-Lamba Cassiterite Toward Effective Tin Oxide Production

## ABSTRACT

Cassiterite has been an essential source of tin; its exploration and exploitation have become a priority worldwide. The effective beneficiation of cassiterite depends mainly on its grindability and effective liberation. The Modified Bond's grindability test is a method used to determine the work index, which is crucial in estimating the energy needed to grind an ore. This is crucial during mineral processing, as a slight deviation would affect the company's operating expenditure (OPEX). This study investigates the work index for Farin-Lamba cassiterite with reference to silica sand sourced from Igbokoda. The test ore (cassiterite) was analyzed using Energy Dispersed X-ray fluorescence spectrometer (ED-XRS), Petrographic Analysis, and Scanning Electron Microscope equipped with an Energy Dispersive Spectrum (SEM-EDS) to understand their chemical and mineralogical characteristics in relation to their grindability. The test ore and the reference material (silica sand) underwent comminution using 500g of each to a 100% passing 500  $\mu\text{m}$  array of sieves arranged in ( $\sqrt{2}$ ) series from 500  $\mu\text{m}$  to 63  $\mu\text{m}$  onto an automatic sieve shaker. The chemical and mineralogical analysis revealed the presence of gangue such as  $\text{SiO}_2$  and  $\text{Al}_2\text{O}_3$ , which increases the energy needed during comminution; further, the presence of rough and large grain size in the ore also increases the energy needed for comminution. The results were subjected to Gaudin Schuman's equation to determine the ore's work index, which was 14.664 KWh/ton for the test ore, which is standard for cassiterite, which ranges from 10-15 kWh/ton. Further, the energy needed for comminution was calculated to be 33.7272 Kwh, providing valuable insights into the energy efficiency of the grinding process. The evaluation of the grindability of Farin-Lamba cassiterite in relation to the reference ore not only contributes toward understanding the ore processing dynamics but also provides information needed for the optimization of energy consumed during the process of tin oxide production.

Keywords: Cassiterite, Characterization, Bonds Equation, Grindability, Work Index, Comminution Optimization, Tin Oxide, Mineralogy, Geochemistry

## 1. INTRODUCTION

Tinstone, also known as cassiterite, is a mineral that is translucent in its pure form but turns brownish-blackish when iron, aluminium, and silica impurities are present. Cassiterite has a 78.6% tin oxide percentage when chemically pure but is generally uncommon. However, when it is impure, the tin content can range from 40 % to 55%. There exist two basic kinds of deposits containing cassiterite; firstly, it is present in veins and fissures in the granite and adjacent parent rocks and is the principal constituent of some late-stage granitic intrusions. Secondly, the deposit occurs in secondary origin and can be found as detrital, placer, or alluvial deposits. Tin oxide ( $\text{SnO}_2$ ) is a substance utilized in many different sectors worldwide, including electronics, ceramics, and coatings, and is a necessary component of modern technology (Angadi et al. 2015; Liu et al. 2011).

Nowadays, the majority of cassiterite's sources are alluvial deposits containing weathered grains rather than primary deposits; Malaysia, Bolivia, Indonesia, Belgium, Congo, and Nigeria account for the majority of the world's supply

36 of tin ore. Cassiterite has been an important source of tin for various metallurgical applications and is still the  
37 greatest source of tin today. The exploitation of mineral resources has become a top priority in many developing  
38 nations, leading to the depletion of high-grade ores (Gitau et al. 2024). Nigeria, for example, has abundant mineral  
39 resources, such as iron ore, manganese, copper, and coal, that have significantly increased the country's gross  
40 domestic product (GDP), bringing about socioeconomic benefits. The production of tin oxide depends on the  
41 efficient beneficiation of cassiterite, which must first go through a comminution process that involves ore crushing  
42 and grinding. Therefore, knowing the ore's grindability is an important step toward the efficient and effective  
43 production of tin oxide (Oyelola et al. 2024).

44 It is essential to understand the geochemistry and mineralogy of minerals as it help address problems associated with  
45 beneficiation and concentration. Thomas et al. (2019) pointed out some crucial attributes that need to be considered,  
46 such as characteristics of the elements in the mineral ore, bulk modal mineralogy, grain size, texture, and  
47 association. These important features are limited and need to be considered as ore mineralogy is a complex and  
48 intricate, but it contribute primarily to deciding the best separation process. Characterizing the element of interest  
49 within the minerals present in the ore to define the elements' entitlement is the first step in identifying the  
50 mineralogical limit to separation. This can be achieved by making use of the combination of the new advanced  
51 automated scanning electron microscopy technique, which helps point out the elemental composition and in-depth  
52 ore characteristics (Alabi, Gbadamosi, and Ola-Omole 2019; Gitau, Maghanga, and Ondiaka 2022)

53 The goal of the comminution circuit in mineral processing is to prepare the ore as a suitable feed for separation  
54 processes, which upgrade the material by rejecting the particles that do not contain economically significant  
55 amounts of the target mineral. Comminution theory deals with the relationship between energy input into particle  
56 size reduction and the particle size distribution from a given feed size. In contrast, grindability tests seek to estimate  
57 the energy consumption of grinding and to give parameters for the grinding mill sizing using various test methods.  
58 The comminution process significantly converts the ore from a population of particles with a relatively uniform  
59 grade to particles with a range of compositions that allow them to be separated into low-grade and high-grade  
60 streams (Angadi et al. 2015; Lehmann 2021).

61 Insufficient mineral liberation during the separation phases of an ore is a result of grinding it to excessively coarse  
62 particle size. However, grinding the mineral too fine results in higher grinding costs and possibly low final recovery.  
63 Thus, efficient grinding is one of the most important components of effective mineral processing. Energy  
64 consumption drives the cost of grinding. Extensive grinding might not always be a disadvantage because the earlier  
65 steps might compensate for the higher energy use. While the primary goal of grinding is to achieve the economic  
66 degree of release, grinding is also occasionally employed to enhance the surface area of minerals (Yang et al. 2021).

67 The most energy-intensive step in mineral processing is grinding, which comes at the end of the comminution  
68 process and can cost a mineral processing plant more than half its operating expenses. The goal of grinding is the  
69 economic degree of liberation of the target mineral. Thus, understanding an ore's comminution qualities is crucial  
70 whether running a mineral processing facility or carrying out a feasibility assessment (Olatunji and Durojaiye 2010).

71 While tumbling mills have reached a high level of mechanical efficiency and dependability, there is ongoing  
72 discussion on their energy efficiency. The main issue with tumbling mills and all other crushing and grinding  
73 equipment is that very little of the energy input is used to break the ore because the equipment consumes the  
74 majority. Less than 1% of the entire energy input is available for size reduction, with most of the energy being used  
75 to produce heat, as demonstrated by Wills et al. (2006).

76 The primary objective of this research is to understand the mineralogical and chemical characteristics and evaluate  
77 the grindability behavior of Farin-Lambacassiterite using the modified Bonds Index for effective beneficiation.  
78 Understanding the grindability and the ore composition can pave the way for the optimization of processing circuits  
79 to enhance sustainable tin oxide production.

## 80 2. MATERIALS AND METHODS

### 81 2.1 Materials

82 The samples for this research came from Farin-Lamba mines, situated in Plateau State, Nigeria's Jos South Local  
83 Government Area, collected from different pits tagged Pit LCA-1, LCA-2, LCA-3, LCA-4, and LCA-5.

### 84 2.2 Methods

85 A Denver Laboratory Milling Machine (D-12) was used to grind the samples to determine their liberation size and  
86 conduct mineralogical and elemental analysis of the crude material. After crushing and grinding, the reference ore,  
87 Igbokoda silica, and the test ore were charged into a set of sieves and left on an automatic sieve shaker for 20  
88 minutes. Weighing the sieve fractions of the test and reference ore that was retained allowed us to record the feed  
89 product's value for work index calculations.

90 The processed samples underwent mineralogical characterization by utilization of an X-ray Diffractometer (XRD)  
91 (Model: PANalytical Minipal 7), a Scanning Electron Microscope equipped with a Dispersion Spectrum (SEM-  
92 EDS) (Model: QEMSCAN), and a Petrological Analyzer (Model: Leica EGB 100). Finally, the modified Bond's  
93 Equation (O. O. Alabi et al. 2015) was used to determine the theoretical work index of cassiterite, which involves  
94 using reference material such as silica whose grindability is known, as shown in Equation 1-2.

$$95 \text{ Wit} = \text{Wir} \left( \frac{10}{\sqrt{P}} - \frac{10}{\sqrt{F}} \right) \quad [1]$$

$$\text{Wit} = \text{Wir} \left( \frac{\frac{10}{\sqrt{Pr}} - \frac{10}{\sqrt{Fr}}}{\frac{10}{\sqrt{Pt}} - \frac{10}{\sqrt{Ft}}} \right) \quad [2]$$

96 Where Wit is the test ore Work Index, Wir is the reference ore Work Index, Pr is the reference ore where 80% of the  
97 materials pass 100µm, Pt is the test ore diameter where 80% of the materials pass 100µm, Fr is the reference ore  
98 diameter where 80% of the feed pass 100µm, Ft is the test ore diameter where 80% of the feed pass 100µm, Wr is  
99 the reference ore work input and Wt is the test ore work input (Valerevich Lvov et al. 2019).

100 **3. RESULT AND DISCUSSION**

101 3.1 Results

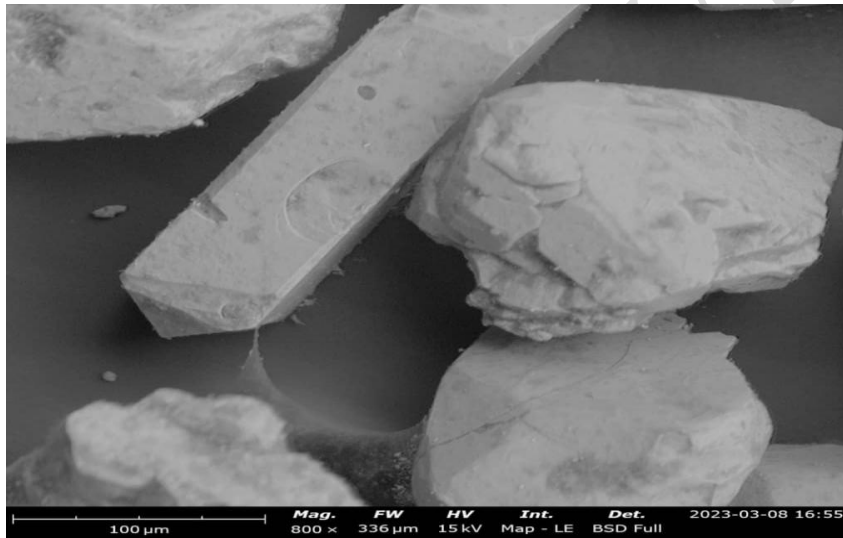
102 3.1.1 Elemental analysis of the cassiterite sample

103 Table 1: Chemical Composition of the Crude Cassiterite

Compounds	Al <sub>2</sub> O <sub>3</sub>	SnO <sub>2</sub>	Ta <sub>2</sub> O <sub>5</sub>	SiO <sub>2</sub>	Fe <sub>2</sub> O <sub>3</sub>	BaO	SO <sub>3</sub>	ZrO <sub>2</sub>	TiO <sub>2</sub>	Nb <sub>2</sub> O <sub>3</sub>	CaO
Composition (%)	5.450	24.720	0.667	49.980	3.500	2.136	1.651	2.550	4.600	1.036	1.785

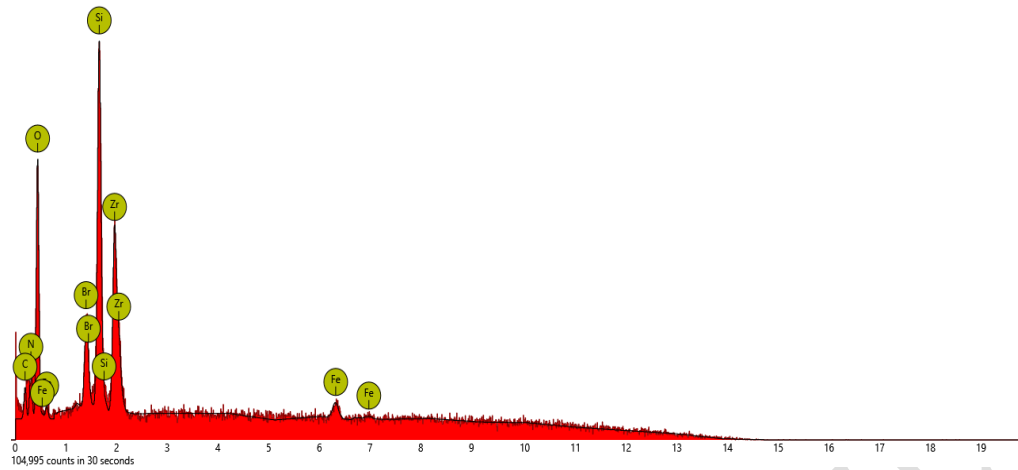
104 3.1.2 Mineralogical characterization examination using a scanning electron microscope with an energy-dispersive spectrum (SEM-EDS)

106 a. SEM micrograph of crude cassiterite



107  
108 Figure 1: Scanned Electron micrograph of crude cassiterite sample

109 b. EDS phase diagram of crude cassiterite



110

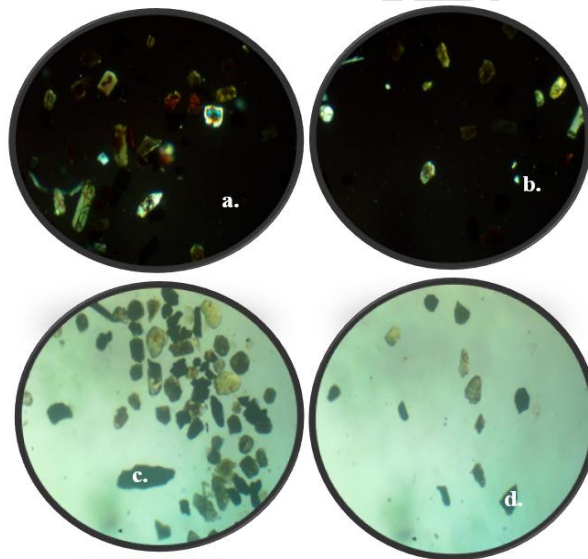
111

Figure 2: EDS of crude cassiterite at 500 μm Magnification

112 3.1.3 Petrological analysis

113 The minerals contained in the test ore were identified using optical techniques in both cross-polarized light (XPL) and plane-polarized light (PPL), as shown in Figure 3.

114



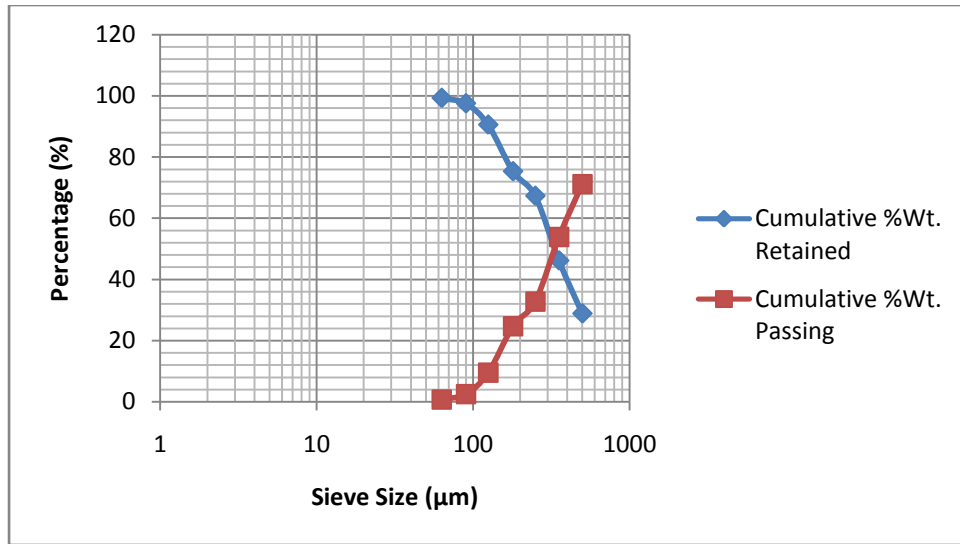
115

116

Figure 3: Petrographs of crude cassiterite at 500 magnification in PPL and XPL

117 3.1.4 Particle Size Analysis

118 The sieve analysis plots of the test (cassiterite) and reference ore (silica sand) feed to the ball mill are displayed in  
 119 Figures 4–7. They plot different varied sieve sizes against the cumulative percentage of the ore retained, and the  
 120 cumulative percentage of the ore passed.

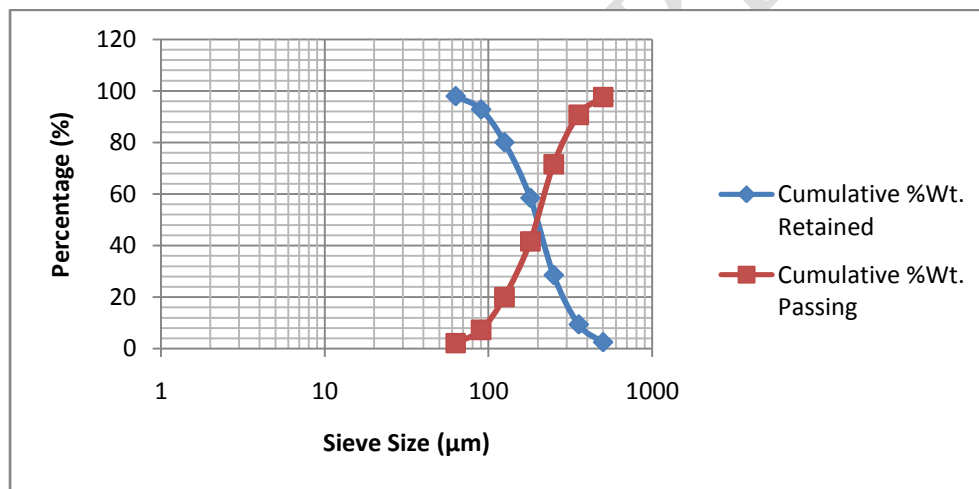


121

122

123

Figure 4: Plot of % cumulative retained and passing against sieve sizes (test ore fed to the ball mill)

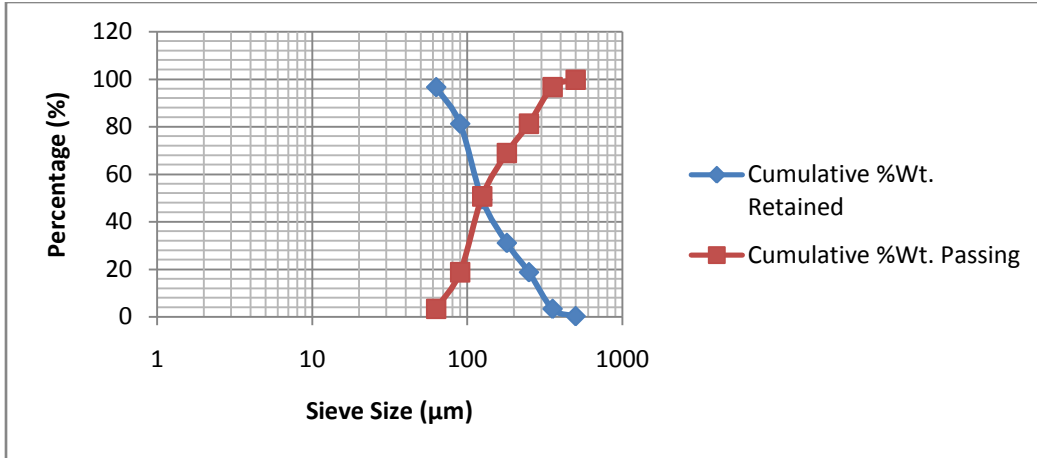


124

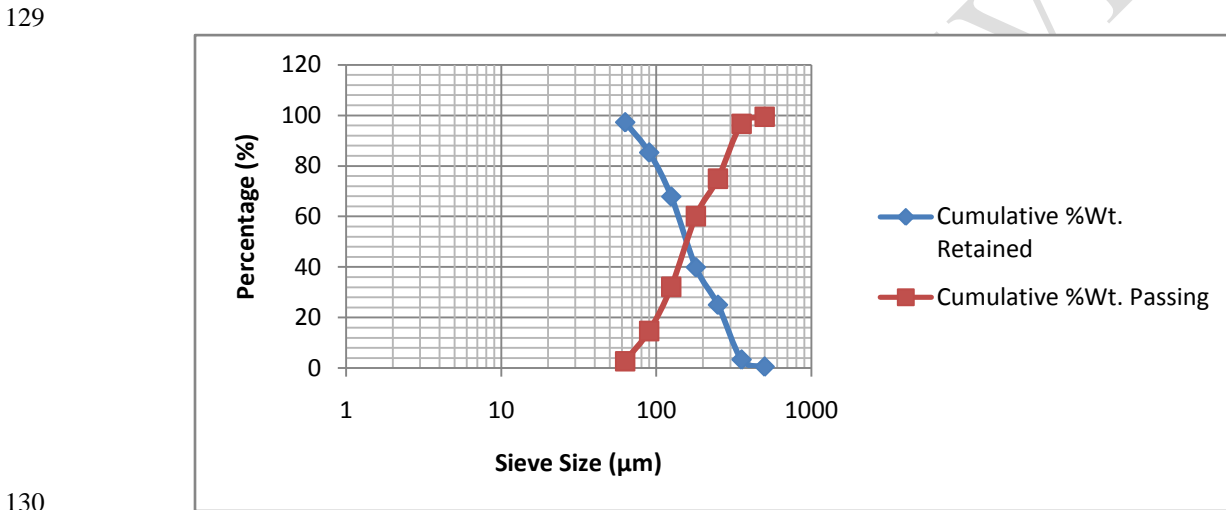
125

126

Figure 5: Plot of % cumulative retained and passing particles against sieve sizes (reference ore fed to the ball mill)



127  
128 Figure 6: Plot of cumulative % retained and passing against sieve sizes (test ore product from ball mill)



130  
131 Figure 7: Plot of cumulative % retained and passing against sieve sizes (reference ore product from ball mill)

132 3.1.5 Grindability Evaluation

133 Equation 4 was used to evaluate the grindability of the cassiterite.

$$R = \frac{F}{P} \tag{4}$$

134 Where R is the reduction ratio, F is the feed particle diameter, and P is the product particle diameter.

135 Utilizing Gaudin Schumann's expression as shown in Equations 5-7;

$$P(X) = 100(X - K)^\alpha \tag{5}$$

$$\alpha = \frac{\log P(X_2) - \log P(X_1)}{\log(X_2) - (X_1)} \tag{6}$$

$$\text{Sieve 1} = \frac{\% \text{ Passing in Sieve 1}}{\% \text{ Passing in Sieve 2}} \times \text{sieve 2} \tag{7}$$

136 Where X is the sieve size with 80% particle passing

137 Table 2: 500 µm and 250 µm mesh sizes of sieves having an 80% particle size pass rate.

Samples	80% Passing Feed µm (F)	80% Passing Milled Product µm (P)
Test Ore (Cassiterite)	592.13	238.66
Reference Ore (Silica Sand)	660.20	250.44

138

139 3.1.6 WorkIndexDetermination

140 According to the literature, the Work Index of Silica sand is between 2.65 Kwh/t - 16.46 Kwh/t (Alabi et al. 2016). Taking  
141 14.1 as the Work Index of Silica sand. Therefore, the determination of the work index involved inputting the values  
142 obtained from Table 1 into Equations 1 and 2, resulting in a Wir of 14.664 KWh/ton.

143 Where  $W_{ir} = 14.1$  Kwh/ton

$$W_{it} = 14.1 \times \left( \frac{10}{\sqrt{\frac{250.44}{10}}} - \frac{10}{\sqrt{\frac{660.20}{10}}} \right) \frac{1}{\sqrt{\frac{238.66}{10}}} = 14.664 \text{ Kwh/ton}$$

144 3.1.7 Energy used during grinding

145 The energy used to obtain the optimal liberation size during the comminution process was determined by substituting the  
146 test work index in Equation 1.

$$W_t = 10 \times 14.664 \times \left( \frac{1}{\sqrt{\frac{238.66}{10}}} - \frac{1}{\sqrt{\frac{592.13}{10}}} \right) = 33.7272 \text{ Kwh}$$

147 3.2 Discussion

148 The chemical composition of the crude cassiterite ore revealed 24.72%  $SnO_2$  (tin oxide), as shown in Table 1, which  
149 is the main mineral of interest. There are also considerable amounts of gangue, such as  $SiO_2$  (49.98%) and  
150  $Al_2O_3$  (5.45%), among others. Elements such as  $SiO_2$  contribute to the formation of hard and abrasive grains due to  
151 the presence of minerals such as quartz that increase the energy needed during comminution and increases also  
152 increase the wear and tear during grinding, thereby reducing the grindability of the cassiterite ore.

153 Figures 1-2 show a SEM image at 100 µm with 800 magnification, as well as an EDS qualitative analysis of the  
154 Farin - Lamba Cassiterite deposit at 500 magnification for Spectrum 1. The SEM morphology reveals that the  
155 minerals in the ore matrix are closely packed, allowing for simple liberation via grinding, which is a key and result-  
156 determining step in mineral processing, and all subsequent downstream processes in the beneficiation chain rely  
157 totally on it (Matsanga, Nheta, and Chimwani 2023). The EDS qualitative analysis of the image revealed that the  
158 primary elemental elements of minerals in the ore matrix are *Fe, Sn, O, K, Ca, Al, and Si*.

159 SEM-EDS examines the composition and microstructure of samples at a scale and gives valuable insights into the  
160 mineralogical composition of the ore, including the distribution of different mineral phases and the presence of  
161 minerals and their gangue constituents in the ore matrix. This information is critical for understanding ore and

162 gangue composition, mineralogy, and texture impact of the grindability of the ore. The presence of abrasive and  
163 coarse minerals within the ore affects its grindability by increasing the energy consumption and wear rates of the  
164 comminution equipment. On the other hand, the absence of such minerals indicates better grindability of the ore.

165 There also exists a relationship between ore petrography (Figure 3) and cassiterite grindability. Petrological analysis  
166 helps to understand various mineralogical associations, such as particle shape and agglomeration within the ore,  
167 which affect liberation. The ore generally displays isotropic characteristics under crossed polarized light  
168 microscopy, revealing subhedral grain shape within a network of Si and Fe intrusions within the host rock. The grain  
169 arrangement also appears to be loosely packed within the ore matrix, justifying the low energy used during grinding.  
170 Though cassiterite exhibits a subhedral shape and generally does not exhibit a complex structure, thus allowing easy  
171 grindability, the presence of silica and iron gangue may consequently affect the grindability and increase the energy  
172 for liberation.

173 Most known minerals occur in consolidated forms, and adequate data on the particle sizes at which these minerals  
174 exist separately is required to allow the separation of the mineral of interest from others. Fractional sieve size  
175 analysis of Farin-Lambacassiterite revealed that 27.78 g of the total 100 g was retained on 500  $\mu\text{m}$ , 16.53 g on 355  
176  $\mu\text{m}$ , 20.36 g on 250  $\mu\text{m}$ , 7.71 g on 180  $\mu\text{m}$ , 14.67 g on 125  $\mu\text{m}$ , 6.71 g on 90  $\mu\text{m}$ , 1.71 g on 63  $\mu\text{m}$ , 0.68 g and -63  $\mu\text{m}$ .  
177 The cumulative percentage passing following the order of sieve arrangement from the coarsest is obtained as 71.14  
178 %, 53.86 %, 32.71 %, 24.7%, 9.46 %, 2.49%, and 0.71%. The obtained weight retained in grams indicates easy  
179 handling and precise results for the laboratory analysis, which is a possibility of separating the particle size fractions.

180 The sieve analysis results revealed that the 80% passing particle size fractions for the reference (Fr) and test ore (Ft)  
181 fed into the ball mill were 632.25  $\mu\text{m}$  and 312.5  $\mu\text{m}$ , respectively, and the 80% passing particle size fractions for the  
182 products that came out of the ball mill were 242.25  $\mu\text{m}$  and 284.55  $\mu\text{m}$ , respectively. The plateau condition Farin-  
183 LambaCassiterite was found to have a work index of 14.664 Kwh/ton and grindability energy of 33.7272 Kwh. This  
184 suggests that reducing one ton of the plateau state Farin-LambaCassiterite from 80% passing size requires 33.7272  
185 Kwh of energy.

#### 186 4. CONCLUSION AND RECCOMENDATIONS

187 Having carried out the experimentation and subsequent discussions. This study has established the viability of the  
188 Farin-Lambacassiterite for tin oxide recovery. From the results obtained, the following inferences were drawn:

- 189 i. The chemical composition analysis shows the presence of tin oxide with the 24.72% assay in the ore; there  
190 are also high amounts of  $\text{SiO}_2$  with a composition of 49.98%, which influences ore grindability.
- 191 ii. SEM/EDS shows the morphological structure of the mineral and its crystallography; this reveals the  
192 distribution of grain minerals in the ore matrix (coarse), mainly quartz. This enhances grindability, hence  
193 reducing the energy needed for effective mineral liberation.
- 194 iii. The petrological analysis shows that the grain particles are loosely packed within the ore matrix,  
195 consequently aiding its grindability. The results complement the SEM-EDS results.

196 iv. Farin-Lambacassiterite work index was computed to be 14.664 Kwh/ton, utilizing a grindability energy of  
197 33.7272 Kwh. The actual work needed to grind an ore is usually less than 1%, as the remaining energy is  
198 dissipated as vibration, noise, and heat (Bouchard et al. 2017). Therefore, this justifies the less energy used  
199 in cassiterite grinding as the ore is brittle and soft, as revealed in the mineralogical characterization. This  
200 parameter serves to help the development of a process for the beneficiation of Farin-Lambacassiterite ore to  
201 the economic and technological development of a nation.

202 Effective beneficiation depends on the use of effective mineral separation processes that are based on the  
203 petrological features of the ore. The utilization of flotation, magnetic separation, and gravity separation techniques  
204 can aid in the focused elimination of gangue minerals, thus increasing the cassiterite concentration. Furthermore,  
205 energy efficiency must be closely monitored throughout the beneficiation process, which calls for a cautious  
206 assessment of the grinding parameters and reduction of heat, noise, and vibration-related energy losses by  
207 optimization. The beneficiation of Farin-Lambacassiterite ore can promote economic development and help achieve  
208 the larger objectives of sustainable resource management and technological advancement by taking a comprehensive  
209 approach that combines technical optimization with environmental care.

#### 210 DATA AVAILABILITY

211 The data used in this research is available upon request.

#### 212 5. REFERENCES

213 Alabi, Oladunni, Yemisi Gbadamosi, and Omoyemi Ola-Omole. 2019. CHEMICAL AND MINERALOGICAL  
214 CHARACTERIZATION OF ITAKPE IRON ORE MINE WASTES (TAILINGS).  
215 <https://www.researchgate.net/publication/364587551>.

216 Alabi, Oladunni Oyelola, Shehu Aliyu Yaro, George Thomas Dungka, Ferdinand Asuke, Binta Hassan. 2016.  
217 Comparative Beneficiation Study of Gyel Columbite Ore Using Double Stage (Magnetic-to-Magnetic and  
218 Magnetic-to-Gravity) Separation Techniques. *Journal of Minerals and Materials Characterization and*  
219 *Engineering* 4 (2). Scientific Research Publishing:181–193. doi:10.4236/JMMCE.2016.42017.

220 Angadi, S. I., T. Sreenivas, Ho Seok Jeon, Sang Ho Baek, and B. K. Mishra. 2015. A Review of Cassiterite  
221 Beneficiation Fundamentals and Plant Practices. *Minerals Engineering* 70. Elsevier Ltd:178–200.  
222 doi:10.1016/J.MINENG.2014.09.009.

223 Bouchard, Jocelyn, gilles LeBlanc, Michelle Levesque, Peter Radziszewski, and David George-Filteau. 2017.  
224 *Breaking down Energy Consumption in Industrial Grinding Mills*.

225 Gitau, Francis, Oladunni Oyelola Alabi, Fatai Olufemi Aramide, Kayode Henry Talabi, and Mary Nelima Ondiaka.  
226 2024. Towards a Sustainable and Enhanced Iron Ore Recovery: Bio-Beneficiation Review. *Mining,*  
227 *Metallurgy and Exploration*. doi:10.1007/s42461-024-00950-2.

228 Gitau, Francis, Justin Kambale Maghanga, and Mary Nelima Ondiaka. 2022. MAPPING AND

229 CHARACTERIZATION OF SOLID IRON ORE MINING WASTES IN KISHUSHE AREA, TAITA  
230 TAVETA COUNTY, KENYA. Taita Taveta University. <http://ir.ttu.ac.ke:8080/xmlui/handle/123456789/80>.

231 Lehmann, Bernd. 2021. Formation of Tin Ore Deposits: A Reassessment. *Lithos* 402–403 (November).  
232 Elsevier:105756. doi:10.1016/J.LITHOS.2020.105756.

233 Liu, Siqing, Ye Cao, Xiong Tong, and Peng Li. 2011. Beneficiation of a Fine-Sized Cassiteritebearing Magnetite  
234 Ore. *Minerals and Metallurgical Processing* 28 (2). Society for Mining, Metallurgy and Exploration:88–93.  
235 doi:10.1007/BF03402393.

236 Matsanga, Nyasha, Willie Nheta, and Ngonidzashe Chimwani. 2023. Grinding Media in Ball Mills–A Review, April.  
237 Preprints. doi:10.20944/PREPRINTS202304.0811.V1.

238 Olatunji, K.J., and A.G. Durojaiye. 2010. Determination of Bond Index of Birnin- Gwari Iron Ore in Nigeria.  
239 *Journal of Minerals and Materials Characterization and Engineering* 09 (07):635–642.  
240 doi:10.4236/jmmce.2010.97045.

241 Oyelola, Alabi Oladunni, Borode Joseph Olatunde, Ajaka Oyedele Ebenezer, and Gbadamosi Yemisi Elizabeth.  
242 2024. Investigating the Gravity Beneficiation Consequence on Farin-Lamba (Plateau State) Cassiterite  
243 towards Tin Oxide Production. *Saudi Journal of Engineering and Technology* 9 (02):121–127.  
244 doi:10.36348/sjet.2024.v09i02.011.

245 Thomas, D.G., F. Asuke, S.A. Yaro, and S.M. Adams. 2019. Chemical, Mineralogical and Petrological  
246 Characterization of Gyaza Iron Ore Deposit, Katsina State, Nigeria. *Nigerian Journal of Technology* 38  
247 (3):660. doi:10.4314/njt.v38i3.17.

248 Valerevich Lvov, Vladislav, Leonid Sergeevich Chitalov, Berry T F, Bruce R W, Horst W E, Bassarear J H,  
249 Shahsavari Sh, Kapur P C, Gharegheshlagh H Hojjat, and Lewis K A. 2019. Comparison of the Different  
250 Ways of the Ball Bond Work Index Determining. *Papers.Ssrn.Com* 10 (3):1180–1194.  
251 [https://papers.ssrn.com/sol3/papers.cfm?abstract\\_id=3452642](https://papers.ssrn.com/sol3/papers.cfm?abstract_id=3452642).

252 Wills, Barry A., and James A. Finch. 2015. *Wills' Mineral Processing Technology: An Introduction to the Practical  
253 Aspects of Ore Treatment and Mineral Recovery*. Wills' Mineral Processing Technology: An Introduction to  
254 the Practical Aspects of Ore Treatment and Mineral Recovery. Elsevier/BH.

255 Yang, Xiaojing, Shaojian Ma, Linling Jiang, and Runnan Guo. 2021. Approach of Establishing the Grinding  
256 Population Balance Kinetic Model for Cassiterite-Polymetallic Sulfide Ore. *Ferroelectrics* 578 (1). Taylor and  
257 Francis Ltd.:66–80. doi:10.1080/00150193.2021.1902764.